Acta Crystallographica Section D
Biological Crystallography
ISSN 0907-4449

Structure of GES-1 at atomic resolution: insights into the evolution of carbapenamase activity in the class A extended-spectrum β-lactamases

Clyde A. Smith,[a]* Marisa Caccamo,[b] Katherine A. Kantardjieff[c] and Sergei Vakulenko[b]

[a]Stanford Synchrotron Radiation Laboratory, Stanford University, Menlo Park, CA, USA, [b]Department of Chemistry and Biochemistry, University of Notre Dame, Notre Dame, IN, USA, and [c]W. M. Keck Foundation Center for Molecular Structure and Department of Chemistry and Biochemistry, California State University Fullerton, Fullerton, CA, USA

Correspondence e-mail: csmith@slac.stanford.edu

Received 24 May 2007
Accepted 28 July 2007

PDB Reference: GES-1, 2qpn, r2qpnsf.

The structure of the class A extended-spectrum β-lactamase GES-1 from *Klebsiella pneumoniae* has been determined to 1.1 Å resolution. GES-1 has the characteristic active-site disulfide bond of the carbapenemase family of β-lactamases and has a structure that is very similar to those of other known carbapenemases, including NMC-A, SME-1 and KPC-2. Most residues implicated in the catalytic mechanism of this class of enzyme are present in the GES-1 active site, including Ser70, which forms a covalent bond with the carbonyl C atom of the β-lactam ring of the substrate during the formation of an acyl-enzyme intermediate, Glu166, which is implicated as both the acylation and deacylation base, and Lys73, which is also implicated as the acylation base. A water molecule crucial to catalysis is observed in an identical location as in other class A β-lactamases, interacting with the side chains of Ser70 and Glu166. One important residue, Asn170, also normally a ligand for the hydrolytic water, is missing from the GES-1 active site. This residue is a glycine in GES-1 and the enzyme is unable to hydrolyze imipenem. This points to this residue as being critically important in the hydrolysis of this class of β-lactam substrate. This is further supported by flexible-docking studies of imipenem with *in silico*-generated Gly170Asn and Gly170Ser mutant GES-1 enzymes designed to mimic the active sites of imipenem-hydrolyzing point mutants GES-2 and GES-5.

1. Introduction

β-Lactams are the most common antibiotics in clinical use and represent more than 60% of the total world consumption of antimicrobial drugs (Livermore & Woodford, 2006). They include penicillins, cephalosporins, monobactams, penems and carbapenems and over 50 antibiotics of this class are available on the market for the treatment of various infections caused by Gram-negative and Gram-positive pathogens (Siu, 2002; Bartlett, 2003; Emsley & Cowtan, 2004; Poole, 2004). The efficacy and low toxicity of β-lactams is directly related to their mechanism of action, namely the inhibition of uniquely bacterial enzymes, the penicillin-binding proteins (PBPs), which are involved in the biosynthesis of the bacterial cell wall.

Over 60 years of extensive and sometimes uncontrolled use of antibiotics has resulted in the selection and worldwide spread of resistant microorganisms and this poses a serious threat to antibiotic therapy of infectious diseases. A major mechanism of bacterial resistance to β-lactam antibiotics, particularly in Gram-negative pathogens, is the production of β-lactamases, enzymes that hydrolyze the conserved four-

Table 1
Data-collection statistics.

Values in parentheses are for the highest resolution shell: 2.0–1.9 Å for the medium-resolution data and 1.05–1.00 Å for the high-resolution data.

	Data set	
	Medium-resolution†	High-resolution‡
Maximum resolution (d_{min}) (Å)	1.9	1.0
Observed reflections	288144	615952
Unique reflections to d_{min}	36180	237028
R_{merge}§ (%)	9.6 (37.5)	4.6 (34.9)
$I/\sigma(I)$	7.3 (2.1)	11.47 (2.69)
Completeness (%)	84.2 (88.4)	93.4 (90.1)
Unit-cell parameters		
a (Å)	42.33	42.41
b (Å)	80.92	80.82
c (Å)	70.86	71.44
β (°)	101.0	101.4

† Processed and scaled with *HKL*-2000. ‡ Processed and scaled with *XDS* and *XSCALE*. § $R_{merge} = \sum|I - \langle I\rangle|/\sum I \times 100$, where I is the the observed intensity and $\langle I\rangle$ is the mean intensity.

membered ring of β-lactams, rendering them inactive (Poole, 2004; Livermore & Woodford, 2006). All known β-lactamases are subdivided into four molecular classes (A, B, C and D; Ambler *et al.*, 1991). Three of them (A, C and D) utilize an active-site serine for catalysis, while class B enzymes are metal-dependent.

Class A enzymes are the most abundant in both Gram-negative and Gram-positive pathogens. Originating as relatively narrow-spectrum enzymes capable of hydrolyzing mostly penicillins and sometimes early (first- and second-generation) cephalosporins, some of them (such as TEM and SHV) have evolved into a large superfamily of extended-spectrum β-lactamases (ESBLs) capable of hydrolyzing modern cephalosporins and monobactams (Jacoby & Bush, 2007). Although hundreds of TEM and SHV ESBLS have been reported in the last 30 years, none of them produce resistance to carbapenem antibiotics. The mechanism of the class A β-lactamases involves the deprotonation of an active-site serine residue (Ser70 using the standard numbering scheme of Ambler *et al.*, 1991) followed by the nucleophilic attack of the β-lactam ring of the antibiotic to produce an acyl-enzyme intermediate. This intermediate is subsequently hydrolyzed by a water molecule which has been activated by a general base. The identity of the catalytic base has not yet been fully resolved. Although it has been established that Glu166 is responsible for the water-mediated deacylation of the acyl-enzyme intermediate (Strynadka *et al.*, 1992), there are two possibilities for the deprotonation of Ser70: either Glu166 acting *via* a water molecule in a proton-shuffling mechanism or Lys73 interacting directly with the serine (Minasov *et al.*, 2002).

The first GES (Guiana extended-spectrum; named after the country of origin of the first isolate) β-lactamase, GES-1, was described in 2000 (Poirel *et al.*, 2000). This ESBL is very distantly related to other class A β-lactamases and produces resistance to penicillins and first-, second- and some third-generation cephalosporins (*e.g.* ceftazidime), but not to monobactams and carbapenems. Since 2000, nine GES-type enzymes (GES-1–GES-9) from different geographical locations have been described (Giakkoupi *et al.*, 2000; Mavroidi *et al.*, 2001; Poirel *et al.*, 2001, 2005; Vourli *et al.*, 2004; Wachino, Doi, Yamane, Shibata, Yagi, Kubota & Arakawa, 2004; Wachino, Doi, Yamane, Shibata, Yagi, Kubota, Ito *et al.*, 2004). The most alarming characteristic of the GES family of enzymes that distinguishes them from the TEM and SHV superfamilies is their apparent ability to evolve into weak carbapenemases, enzymes that are capable of hydrolyzing carbapenem antibiotics. Their potential to produce even higher levels of resistance to virtually all known β-lactam antibiotics, combined with their ability to spread among various microorganisms (almost all GES-type enzymes are associated with integrons), elevate the GES β-lactamases to a recognized resistance threat. Here, we report the first crystal structure of a GES-type ESBL, GES-1 β-lactamase, at atomic resolution.

2. Experimental procedures

2.1. Cloning and protein purification

The nucleotide sequence of the GES-1 β-lactamase gene was optimized for *Escherichia coli* codon usage and the gene was custom-synthesized. Unique *Nde*I and *Hin*dIII restriction-endonuclease sites were introduced at the 3′ and 5′ ends of the gene, while corresponding sites within the protein-coding region were abolished without changing the amino-acid sequence of the enzyme. The gene was cloned between the *Nde*I and *Hin*dIII sites of the expression vector pET24a+ (Novagen) and retransformed into *E. coli* BL21 (DE3) competent cells. For protein purification, bacteria were grown overnight at 310 K with shaking in 50 ml LB medium supplemented with 30 μg ml^{-1} kanamycin A. The bacterial suspension was diluted 50-fold into a total of 1.2 l fresh LB medium supplemented with 30 μg ml^{-1} kanamycin A and the expression of GES-1 β-lactamase was induced with IPTG (0.4 m*M*) when the cells reached an OD_{600} of 0.6. The induced culture was incubated overnight at 298 K with shaking and the bacteria were pelleted at 277 K by centrifugation at 4500*g* for 15 min. Cells were resuspended in 30 ml buffer *A* (20 m*M* Tris pH 7.5), disrupted by sonication for 15 min and centrifuged at 24 000*g* for 40 min. The supernatant was loaded onto a Macro-Prep DEAE Support anion-exchange column equilibrated with buffer *A*. The column was washed with 200 ml buffer *A* and the proteins were eluted with a linear gradient of NaCl (0–1 *M* NaCl). Fractions were analyzed by SDS–PAGE and by their ability to turn over chromogenic cephalosporin nitrocephin. Those fractions containing the desired activity were pooled, concentrated to a volume of 20 ml and dialyzed against buffer *C* (20 m*M* MES pH 5.5). The protein was loaded onto a Macro-Prep High S Support cation-exchange column equilibrated with buffer *C*. The column was washed with 200 ml buffer *C* and the protein was eluted with a linear gradient of NaCl (0–1 *M* NaCl). Fractions containing GES-1 protein were pooled, concentrated to a volume of 20 ml and dialyzed against 20 m*M* HEPES buffer pH 7.6. The enzyme

was further concentrated to a volume of 3.8 ml and its concentration was determined to be 5.5 mg ml^{-1}. The enzyme was more than 95% pure as judged by SDS–PAGE.

2.2. Crystallization and data collection

Initial crystallization trials were set up using Crystal Screens I and II (Hampton Research). Small block-like crystals were observed in condition No. 7 from Crystal Screen II (unbuffered 10% PEG 1000 and 10% PEG 8000) and one of these crystals was frozen in a cryoprotectant comprising the well solution and 10% ethylene glycol. The crystal, which belonged to space group $P2$ or $P2_1$ with unit-cell parameters a = 42.3, b = 80.9, c = 70.9 Å, β = 101.0°, diffracted to approximately 2.0 Å resolution. The Matthews coefficient (Matthews, 1968) assuming two molecules in the asymmetric unit is 2.67 Å^3 Da^{-1} (54% solvent content). A complete data set comprising 180 images with an oscillation angle of 1° was collected from this crystal on beamline BL7-1 at the Stanford Synchrotron Radiation Laboratory (SSRL) using X-rays at 12 670 eV (0.9785 Å). The images were processed with *HKL*-2000 (Otwinowski & Minor, 1997). The final data set containing 36 180 reflections had an $R_{\rm merge}$ of 0.096 to 1.9 Å resolution.

Additional fine screens around the initial hit produced larger crystals with the same morphology. A complete data set to 1.0 Å resolution was collected from one of these crystals on beamline BL11-1 at SSRL using X-rays at 15 000 eV (0.82653 Å). The data were collected in two passes of 350 images with an oscillation angle of 0.3° using the same crystal-to-detector distance: a high-resolution pass with an exposure time of 25 s and a low-resolution pass with an exposure time of 5 s and 80% X-ray beam attenuation, in order to measure reflections that were overloaded in the high-resolution pass. The two data sets were processed, scaled and merged using the programs *XDS* and *XSCALE* (Kabsch, 1993), giving a final data set containing 345 560 unique reflections with an $R_{\rm merge}$ of 0.046 to 1.0 Å resolution. Additional data-collection and processing statistics are given in Table 1.

2.3. Structure solution and refinement

The GES-1 sequence was aligned with the sequences of several other class A β-lactamases of which the structures had been determined. The pairwise sequence identities ranged from 25.4% (PER-1, PDB code 1e25) to 38.2% (KPC-2, PDB code 2ov5). The β-lactamase from *Proteus vulgaris* K-1 (PDB code 1hzo) was chosen as the starting model for molecular replacement because the GES-1 and K-1 enzymes differ in length by only one residue (not including the C-terminus) at position 116, where GES-1 has an insertion of a histidine residue in a loop. The residues which were conserved in the two sequences were retained in the model and those which differed were truncated to alanine. Both primitive monoclinic space groups were tested and two independent molecules were located using the program *MOLREP* from the *CCP*4 suite (Collaborative Computational Project, Number 4, 1994) and the medium-resolution data set in space group $P2_1$, with an R factor of 0.53 and a score of 0.34.

The GES-1 structure was initially refined against the medium-resolution data using *REFMAC* (Murshudov *et al.*, 1999); the initial R factor and $R_{\rm free}$ were 0.454 and 0.507, respectively, for data between 20.0 and 2.5 Å resolution. Three rounds of manual model building with *Coot* (Emsley & Cowtan, 2004), in which the side chains were added according to the GES-1 sequence, followed by TLS and restrained positional and isotropic temperature-factor refinement lowered the R factor and $R_{\rm free}$ to 0.228 and 0.289, respectively, for data between 10.0 and 2.0 Å resolution. The partially refined GES-1 model was then used as the starting model for *SHELX*-97 (Sheldrick & Schneider, 1997) refinement against the atomic resolution data, interspersed with manual model building with *Coot*. The displacement parameters of all atoms were refined anisotropically and a number of side chains were modeled with alternate conformations. For some residues it was possible to model radiation damage, particularly in the Cys63–Cys233 disulfide bond in both molecules. To model both disorder and radiation damage, the site occupancies of the affected atoms were refined in conjunction with the anisotropic displacement parameters. H atoms were added in riding positions in the final *SHELX* cycle. The final R factor and $R_{\rm free}$ were 0.133 and 0.182, respectively, for all data between 10.0 and 1.1 Å resolution.

2.4. Flexible docking

Imipenem was built in *ACD/ChemSketch* 10.00 and exported as a `.mol` file for import into *ICM-Pro* 3.4-9d (Schapira, Abagyan *et al.*, 2003; Schapira, Raaka *et al.*, 2003). Flexible docking of imipenem to GES-1 β-lactamase, as well as G165N and G165S mutants, was performed using *ICM-Pro*, which was also used for the *in silico* mutagenesis of Gly165 to asparagine and serine, respectively. *ICM PocketFinder* (Park *et al.*, 2005), which detects cavities of sufficient size to bind small-molecule ligands, was used to identify and define the receptor 'target' region for docking, as well as to reaffirm the character of the active site accommodating the substrate. The sulfate ion and all solvent molecules with the exception of the hydrolytic water were removed from the defined receptor.

The atomic coordinates and structure factors for GES-1 were deposited in the Protein Data Bank with code 2qpn. Superpositions were performed using the *SSM* procedure (Krissinel & Henrick, 2004) as implemented in *Coot* (Emsley & Cowtan, 2004) and the program *LSQKAB* from the *CCP*4 suite (Collaborative Computational Project, Number 4, 1994). Figures were generated using *PyMOL* (DeLano, 2002).

3. Results and discussion

3.1. The final model

For the description and discussion of the GES-1 structure, the standard numbering scheme for class A β-lactamases outlined by Ambler *et al.* (1991) will be used to allow direct comparison between enzymes. A sequence alignment of GES-

1 with several other class A β-lactamases (Fig. 1) indicates the conversion between the real GES-1 residue numbering and the standard Ambler scheme. The final atomic resolution model consists of two independent molecules: molecule *A* comprising 265 amino acids (residues Lys26–Thr293) and molecule *B* comprising 266 amino acids (residues Ser24–Ser292). The protein model has a geometry close to ideal, with r.m.s.d.s of 0.013 and 0.032 Å for bond lengths and 1–3 distances, respectively. A Ramachandran plot shows that 92.8% of the residues lie in the most favored regions, with a further 7% in the additionally allowed regions. No residues are in disallowed regions. The structural anisotropy of the model was analyzed using the *PARVATI* server (Merritt, 1999). The mean anisotropy of the protein model was 0.385 with a standard deviation of 0.135, which conforms reasonably well with the standard mean anisotropy and standard deviation of 0.45 and 0.150, respectively (Merritt, 1999). Additional refinement statistics are given in Table 2 and representative electron density for the protein is shown in Fig. 2.

The two molecules in the asymmetric unit are related by a noncrystallographic twofold rotation axis and form a loose dimer, with the total surface area buried per monomer being around 900 Å^2. The intermolecular interface between the two monomers is highly hydrated (Fig. 2*a*) and there are numerous additional water-mediated intermolecular interactions. Superposition of the two independent molecules shows that they are essentially identical in structure, with an r.m.s. difference in atomic positions of 0.35 Å for 264 matching C$^\alpha$ atoms.

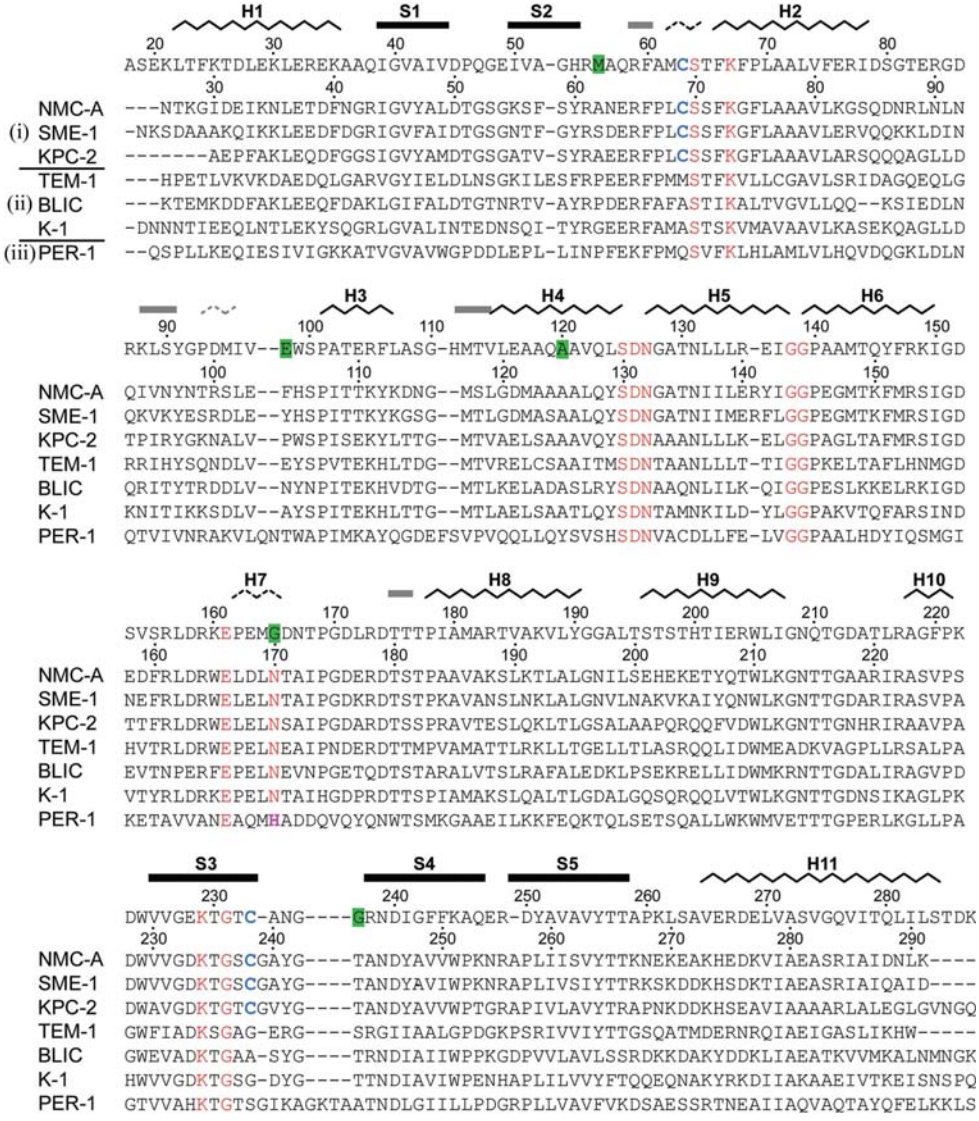

Figure 1
Sequence alignment of GES-1 (top row) with seven class A β-lactamase sequences representing the (i) carbapenemase, (ii) penicillinase and (iii) cephalosporinase subfamilies. The *ges-1* gene-sequence numbering (GenBank code AAF27723) is shown above the GES-1 sequence, along with the secondary-structure elements derived from the current structure. The standard Ambler residue-numbering scheme based upon the TEM-1 sequence (Ambler *et al.*, 1991) is given between the GES-1 and NMC-A sequences and this numbering scheme is used throughout this article. The histidine residue at GES-1 position 111 is an insertion relative to the standard Ambler sequence and is named His116a in the text. Residues in red are fully conserved across the entire β-lactamase family, except for the residue at Ambler position 170, which is histidine in the cephalosporinases and asparagine in all other enzymes. The two cysteine residues specific to the carbapenemases are shown in cyan. Residues in the GES-1 sequence with a green background are those which are point mutations giving rise to other members of the GES subfamily.

3.2. The GES-1 monomer

Each GES-1 monomer is structurally similar to other class A β-lactamases, as expected. The enzyme is folded into two structural domains. Domain 1 comprises residues 26–62 and 218–293, and consists of a five-stranded antiparallel β-sheet with two helices (H1 and H11) packed against the outer face of the sheet (Fig. 3). Domain 2 is folded from a contiguous piece of polypeptide (residues 63–217) and is essentially a globular α-domain consisting of seven α-helices which packs against the concave face of the domain 1 β-sheet. Two short antiparallel β-strands project away from the globular core of domain 2 and are linked by a short 3_{10}-helix and an α-helix (H3).

Table 3 shows the results of the superposition of GES-1 onto several class A β-lactamases chosen to be representative of the three major groupings: (i) the carbapenemases NMC-A and SME-1, (ii) the penicillinases TEM-1, BLIC and K-1 and (iii) the cephalosporinase PER-1. The

Table 2
Structure-refinement statistics.

Resolution range (Å)	10.0–1.1
R factor/R_{free}† (%)	13.30/18.21
R_{all}‡ (%)	13.54
Total atoms: protein/solvent	4135/728
Residues with alternate conformations	25
Residues showing radiation damage§	21
B factors (Å^2)	
Chain A	15.8
Chain B	15.5
Solvent	33.5
R.m.s. deviation from ideality	
Bonds (Å)	0.013
1–3 distances (Å)	0.032
Estimated coordinate error¶ (DPI)	0.032
Overall figure of merit (FOM)	0.912
Mean anisotropy/standard deviation	
Protein atoms	0.385/0.135
Solvent molecules	0.413/0.143
Ramachandran plot: residues in most favored regions (%)	92.8

† $R = \sum ||F_o| - k|F_c|| / \sum |F_o| \times 100$. R_{free} was calculated with 5% of the reflections. ‡ Final R factor calculated with all data using no σ cutoff. § Comprising Comprising 16 acidic residues, four Cys residues and one Met residue. ¶ The Cruikshank diffraction-component precision index.

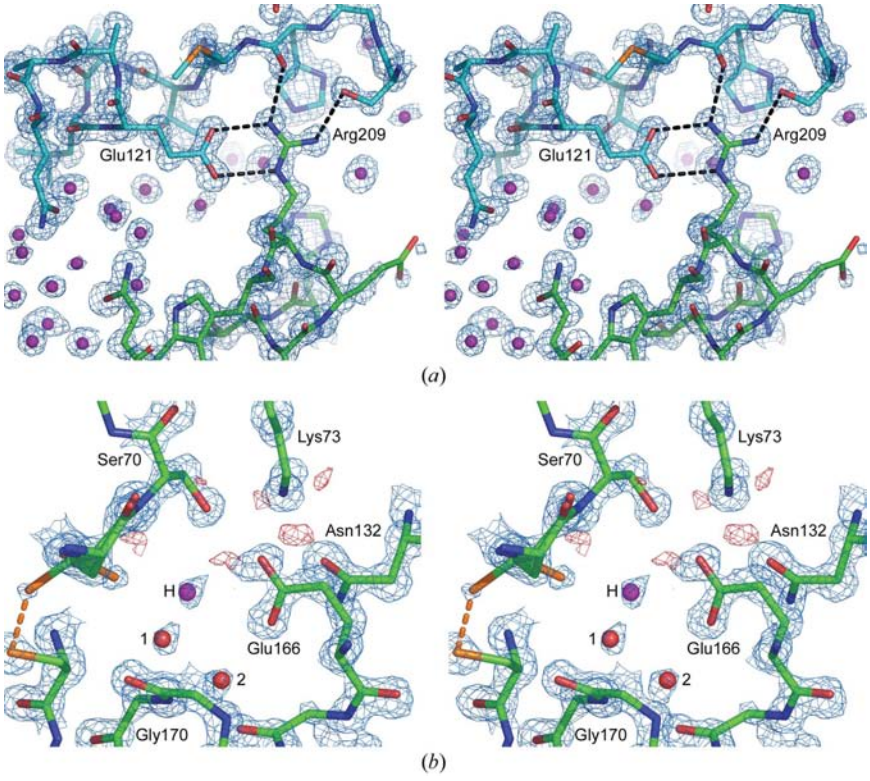

Figure 2
Stereoviews of the final $2F_o - F_c$ electron density (blue, contoured at 1.75 σ). (*a*) The intermolecular interface, showing molecule *B* (cyan sticks) and molecule *A* (green sticks). There are eight direct protein–protein interactions between the two molecules: two salt bridges between Arg111 and Asp218 and between Arg209 and Glu121 (the latter indicated in this figure), two additional hydrogen-bonding interactions from the side chain of Arg209 to Ser115 O$^{\gamma}$ and the carbonyl O atom of His116a (see Fig. 1 for an explanation of the numbering of this residue) and a pair of hydrogen bonds across the noncrystallographic dyad involving Gln215 (not shown). (*b*) The active site of molecule *B*, showing residues Ser70, Lys73, Asn132 and Glu166. The position of the hydrolytic water molecule (H) is indicated by a magenta sphere. Residual $F_o - F_c$ density (red, contoured at 2.0 σ) is visible adjacent to some of the atoms. The $F_o - F_c$ density between the hydrolytic water molecule and the side chain of Glu166 is attributed to the presence of a H atom on the glutamate side chain. Two water molecules (labeled 1 and 2) near Gly170 occupy the position of the asparagine side chain in most other β-lactamases.

r.m.s.d.s for all matching C$^{\alpha}$ atoms range from 1.1 to 1.8 Å. When external loops are omitted, the structural fit is improved, indicating that the core region of GES-1, comprising the domain 1 β-sheet and the domain 2 α-helices, closely matches that of other class A β-lactamases. The largest structural deviations occur in the two terminal helices (H1 and H11), in a strand–helix–strand motif which follows the first helix (H2) in domain 2, at the loops connecting strands S1 and S2 and helix H10 and strand S3 and at the three loops linking secondary-structural elements in domain 1. As expected, the locations of these structural variations correlate with the average temperature factor and the accessibility of the residues, whereby regions of high variability between the structures are at the molecular surface.

3.3. The active site

The active site is located in the cleft formed at the interface of the two domains. The structural disposition of the catalytic residues in GES-1 resembles those in other class A β-lactamases, consisting of the catalytic serine residue Ser70, Lys73 and Glu166, along with an oxyanion hole formed by the main-chain amide N atoms of Ser70 and Thr237. Ser70 is located on a short piece of 3_{10}-helix at the N-terminus of helix H2 in domain 2. Lys73 is located on the first turn of this helix and the side chain projects back towards the active site, forming a hydrogen bond with Ser70 O$^{\gamma}$. An Ω-loop, a highly conserved motif in the β-lactamases, comprising residues 159–182, contains Glu166 and a conserved *cis*-peptide linkage between residues 166 and 167. Adjacent to the active site is a disulfide bond between Cys69 and Cys238. This disulfide, which is characteristic of the carbapenemases, links the N-terminus of helix H2 with the C-terminus of β-strand S3 in domain 1. Superposition of GES-1 with the disulfide-containing carbapenemases (NMC-A, SME-1 and KPC-2) and a number of penicillinases and cephalosporinases which do not have this disulfide indicates that helix H2 of the carbapenemases is positioned slightly closer to domain 1 than in the other enzymes. The presence of this rigid linker could make the enzymes less flexible to some degree and serve to close the active-site cleft somewhat, although the relevance of this to the activity of the enzyme is difficult to ascertain.

The hydrolytic water molecule is also conserved; however, during refinement

it was noted that the occupancy of this water molecule in one of the GES-1 molecules was best modeled as less than unity (~80% in molecule *A*). The water molecule appeared in both molecules only in later stages of the refinement as a peak in $F_o - F_c$ difference Fourier maps and was not as well defined as other nearby water molecules. A second highly conserved water molecule, also with a refined occupancy less than unity (40% in monomer *A* and 65% in monomer *B*), occupies the oxyanion hole between helix H2 and strand S3, interacting with the amide N atom and carbonyl O atom of Thr237, Ser70 O^{γ} and a sulfate anion. The sulfate forms hydrogen-bonding interactions with the side chains of Ser130, Lys234, Thr235, Thr237 and Arg244. Whereas the lysine residue is highly conserved in all β-lactamases, the presence of Arg244 in GES-1 is intriguing. In the other carbapenemases, the equivalent residue is an alanine and the second positively charged side chain is contributed by an arginine residue at position 220. In GES-1 the equivalent residue is a threonine. In this regard, the anion-binding pocket in GES-1 more resembles the pocket in the penicillinases than the carbapenemases.

This positively charged site plays a role in binding the carboxylate group of β-lactamase substrates, including imipenem in TEM-1 (Wang *et al.*, 2002), penicillin G in TEM-1 (Strynadka *et al.*, 1992) and benzylpenicillin, cephaloridine and clavulanic acid in *Staphylococcus aureus* β-lactamase PC1 (Chen & Herzberg, 1992, 2001). Moreover, a sulfate anion is observed in an almost identical position in other class A β-lactamases, including TEM-1 (Jelsch *et al.*, 1993) and PER-1 (Tranier *et al.*, 2000), and this site also binds the carboxylate group of bicine in KPC-2 (Ke *et al.*, 2007) and the sulfonate moiety of MES buffer in the ESBL from *P. vulgaris* K-1 (Nukaga *et al.*, 2002). The presence of the sulfate anion in GES-1 was somewhat surprising, given that at no stage during protein purification were any buffers used that contained sulfate. This could mean that the anion bound adventitiously during bacterial growth and protein expression and was not removed during purification. It is also possible that it could be the sulfonate moiety of either HEPES or MES buffer, since both buffers were used during the latter stages of purification. MES or HEPES buffer molecules have been observed in this site in the ESBL from *P. vulgaris* K-1 (Nukaga *et al.*, 2002) and SHV-2 (Nukaga, Mayama *et al.*, 2003).

One notable residue missing from the GES-1 active site is the highly conserved asparagine at position 170 on the Ω-loop. In the class A β-lactamases, the side chain of Asn170 is the third ligand of the hydrolytic water molecule. The residue at this position in GES-1 is a glycine. Two water molecules fill the vacancy and lie between 1.3 and 1.5 Å from the positions which would normally be occupied by the $O^{\delta1}$ and $N^{\delta2}$ atoms of an asparagine side chain. The two water molecules form hydrogen-bonding interactions with the carbonyl O atoms of Pro167 and Thr237, respectively, and one makes a hydrogen bond with the hydrolytic water. The hydrolytic water molecule is therefore only anchored by hydrogen bonds to the side chains of Ser70 and Glu166. This lack of an additional stabilizing interaction may be the reason why this water molecule is observed with an occupancy of less than unity.

Although the resolution of the refinement was limited to 1.1 Å, it was possible to identify some of the H atoms in the well ordered parts of the GES-1 structure, particularly on the C^{α} atoms. Furthermore, H atoms were also observed on some of the residues in the vicinity of the active site (Fig. 2*b*). Residual $F_o - F_c$ electron density between the hydrolytic water molecule and one of the O atoms of the Glu166 side chain was attributed to the presence of a H atom on the glutamate. This is consistent with the 0.85 Å resolution study of TEM-1 β-lactamase (Minasov *et al.*, 2002), where the pH of crystallization was 8.0 yet a proton was clearly visible in the residual $F_o - F_c$ density maps. The exact pH of crystallization of GES-1 is not known (the crystallization solution was unbuffered); however, it is possible to simulate the

Table 3
Comparison of GES-1 with other representative class A β-lactamases.

The lactamases compared are the carbapenemases NMC-A from *Enterobacter cloacae* (Swaren *et al.*, 1998) and SME-1 from *Serratia marcescens* (Sougakoff *et al.*, 2002), the penicillinases TEM-1 from *Escherichia coli* (Jelsch *et al.*, 1993), BLIC from *Bacillus licheniformis* (Knox & Moews, 1991) and K-1 from *Proteus vulgaris* (Nukaga *et al.*, 2002) and the cephalosporinase PER-1 from *Pseudomonas aeruginosa* (Tranier *et al.*, 2000).

	NMC-A	SME-1	TEM-1	BLIC	K-1	PER-1
PDB code	1bue	1dy6	1btl	1ong	1hzo	1e25
Sequence identity† (%)	35.2	38.1	36.0	32.8	35.9	25.4
R.m.s.d. values‡ (Å)						
All matching C^{α}	1.2 (244)	1.2 (250)	1.3 (256)	1.1 (238)	1.2 (248)	1.8 (244)
Core C^{α}	0.80	0.76	0.90	0.67	0.76	0.93

† Not including the leader sequence. ‡ Values in parentheses give the total number of C^{α} atoms matched. The core (130 C^{α} atoms) comprises residues 42–48, 70–87, 119–165, 179–193, 198–216, 230–237, 243–250 and 259–266.

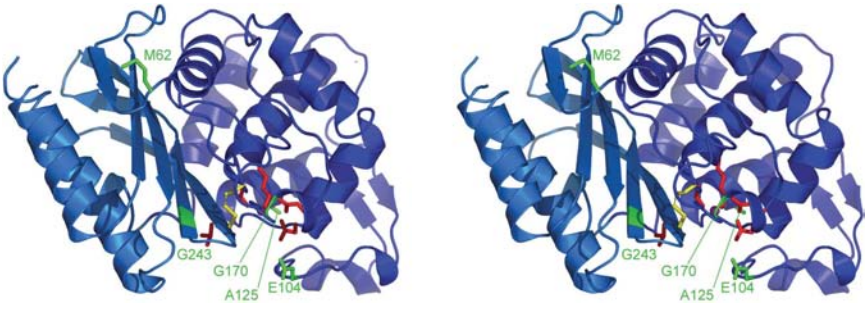

Figure 3
Ribbon representation of the GES-1 monomer showing the two structural domains: domain 1 (left, light blue) and domain 2 (right, dark blue). The locations of the point mutations in other GES-type β-lactamases are indicated as green sticks, except for Gly170 and Gly243, where the loop and the β-strand, respectively, are colored green. Some of the critical catalytic residues are shown as red sticks and the disulfide is shown as yellow sticks. The hydrolytic water molecule is shown as a magenta sphere.

conditions in the crystallization drop by mixing equal volumes of unbuffered 10% PEG 8000/10% PEG 1000 and 20 m*M* HEPES pH 7.6. The pH of this solution was measured at around 7.1. Although this implies that Glu166 should be ionized, it is conceivable that localized changes in the pK_a could give rise to partial protonation of this residue. Moreover, the presence of a proton on Ser70 of SHV-2 (Nukaga, Mayama *et al.*, 2003) but not on Glu166, despite these crystals being grown at pH 7.0, suggests that there is something much more subtle occurring in the active site of the β-lactamase enzymes that cannot be simply explained by consideration of the pH of the external solution.

3.4. Radiation damage and structural disorder

Longer than normal exposure times were necessary to collect atomic resolution data and inevitably the protein became damaged by the high X-ray flux incident on the crystal. The effects of radiation damage in the β-lactamases have been described in detail previously (Minasov *et al.*, 2002; Nukaga, Abe *et al.*, 2003; Nukaga, Mayama *et al.*, 2003; Chen *et al.*, 2005) and similar patterns of damage are seen in GES-1. Briefly, radiation damage to a number of residues is observed, including glutamates, aspartates and methionines. In order to distinguish between atoms missing owing to radiation damage and those missing owing to thermal disorder, the residues in question were compared between the atomic resolution electron-density maps and the maps derived from the model refined at medium resolution, where radiation damage was deemed to be minimal (3.4×10^6 Gy) as calculated by the program *RADDOSE* (Murray *et al.*, 2004) compared with an absorbed dose limit of 3×10^7 Gy (Owen *et al.*, 2006). Only those residues which showed appreciable loss of electron density compared with the 'undamaged' structure were treated as radiation-damaged. Seven acidic residues in molecule *A* and nine in molecule *B* showed varying degrees of decarboxylation, as judged by the refined site occupancies from *SHELX*.

The effects of radiation damage were particularly evident in the two disulfide bridges (Figs. 4*a* and 4*b*). The residues at positions 69 and 238 which correspond to the disulfide cysteines in GES-1 were truncated to alanine during molecular replacement. In the initial stages of the refinement, it was evident from the $F_o - F_c$ electron density that there were at least two conformers for both residues. For residue 238 there was a major peak with a smaller peak attached to the side, readily modeled as two different rotamer conformations for the cysteine residue. The major conformer placed the S^γ atom in an orientation directed towards residue 69. Residue 69 in both GES-1 molecules had two distinct peaks in the $F_o - F_c$ density: a major peak attached to the main-chain $2F_o - F_c$ density near the C^α atom of the alanine and a smaller peak between this C^α and the S^γ atom of residue 238. When residue 69 was mutated to cysteine and the S^γ atom positioned in this second peak, a conventional disulfide linkage with Cys238 was formed. The major conformation could not be modeled with a simple change of rotamer; the entire Cys69 residue had to be repositioned as shown in Figs. 4(*a*) and 4(*b*). The S^γ atom of this conformer is between 1.7 and 1.9 Å closer to the Cys69 main chain. Refinement of the Cys69 occupancies with *SHELX* showed that the occupancy of the conformer involved in the disulfide bond had decreased by over 50% (occupancies were 0.42 and 0.38 in molecules *A* and *B*, respectively). The occupancy of the main rotamer of Cys238 refined to 0.59 and 0.60 for molecules *A* and *B*, respectively.

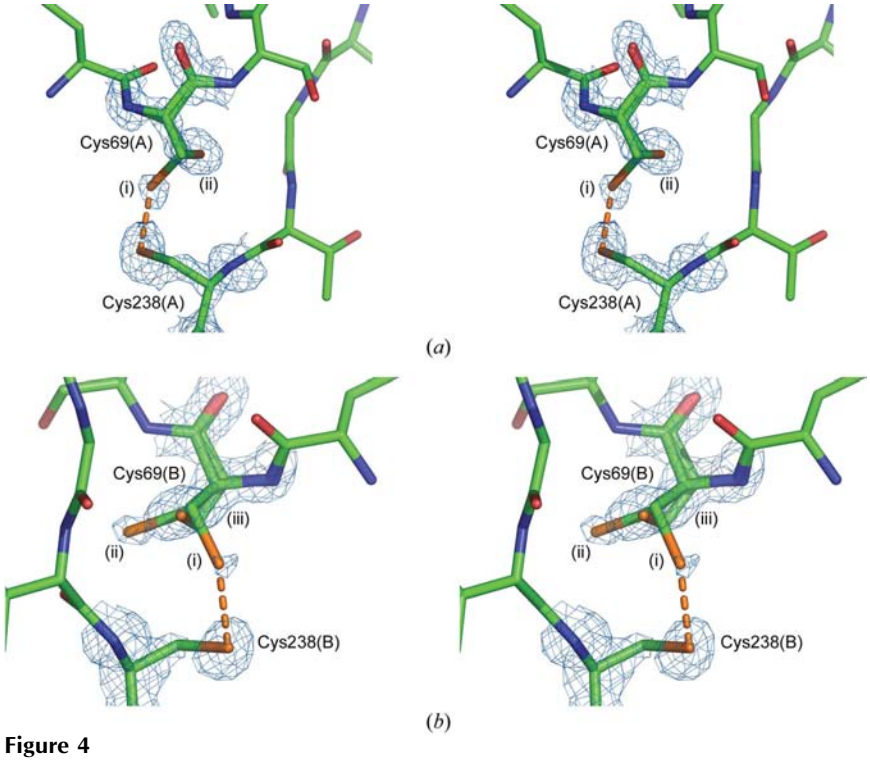

Figure 4
Radiation damage at the active-site disulfide. (*a*) Partial breakage of the disulfide bond in molecule *A*. Two alternate conformations of Cys69 can be seen: the major component is labeled (i) and the minor component, which required a rearrangement of the whole residue, is labeled (ii). A second conformation of Cys238 was also indicated in $F_o - F_c$ electron-density maps but is not indicated in this model. (*b*) Partial breakage of the molecule *B* disulfide, showing three possible conformations of Cys69. The two $C^\alpha - C^\beta$ rotamers are labeled (i) and (ii) and the conformation resulting from a rearrangement of the whole residue is labeled (iii). The $2F_o - F_c$ electron density is contoured at 1.25σ so that the lower occupancy peaks can be seen.

3.5. The GES-type family of β-lactamases

It has been suggested that the class A β-lactamases can be categorized into three subfamilies based upon their preferred substrates and, to a lesser extent, their amino-acid sequences (Tranier *et al.*, 2000). The three families are the penicillinases, of which TEM-1 and SHV-1 are archetypal members, the carbapenemases, which

Table 4
Amino-acid substitutions and activity of the GES-type β-lactamases.

The K_m and k_{cat} values given in this table were derived from the original references describing the isolation and characterization of the GES enzymes and may not be directly comparable since experimental design differs from study to study. The original references are GES-1, Poirel *et al.* (2000); GES-2, Poirel *et al.* (2001); GES-3, Wachino, Doi, Yamane, Shibata, Yagi, Kubota, Ito *et al.* (2004); GES-4, Wachino, Doi, Yamane, Shibata, Yagi, Kubota & Arakawa (2004); GES-5, Bae *et al.* (2007); GES-7, Giakkoupi *et al.* (2000); GES-9, Poirel *et al.* (2005). ND, activity not detected owing to high K_m. NH, no hydrolysis detected. NM, not measured.

	Ceftazidime		Imipenem		Point mutations in the GES enzymes†				
	K_m (μM)	k_{cat} (s^{-1})	K_m (μM)	k_{cat} (s^{-1})	62	104	125	170	243
GES-1	2000	380	45	0.003	Met	Glu	Ala	Gly	Gly
GES-2	>3000	ND	0.45	0.004	—	—	—	Asn	—
GES-3	990	23	NH	NH	Thr	Lys	—	—	—
GES-4	1500	2.5	4.7	0.38	Thr	Lys	—	Ser	—
GES-5‡	394	0.3	4.2	1.2	—	—	—	Ser	—
GES-6‡	NM	NM	NM	NM	—	Lys	—	Ser	—
GES-7§	594	NM	NM	NM	—	Lys	Leu	—	—
GES-8¶	NM	NM	NM	NM	—	—	Leu	—	—
GES-9	>1000	>50	NH	<0.01	—	—	—	—	Ser

† Point mutations are given based upon the GES-1 sequence. Where the sequence is the same as GES-1, this is indicated by a dash. ‡ GES-5 and GES-6 were originally named GES-3 and GES-4, but confusion in the naming led to a reassignment of these names (Lee & Jeong, 2005). § Originally named IBC-1 (Giakkoupi *et al.*, 2000). ¶ Originally named IBC-2 (Mavroidi *et al.*, 2001).

include NMC-A, SME-1 and KPC-2, and the cephalosporinases, such as PER-1. Based purely upon amino-acid sequence, the penicillinases and carbapenemase appear to group together, with sequence identities ranging from 35% to 40%, whereas the cephalosporinases seem to be outliers, with sequence identities in the low- to mid-20% range when compared with the penicillinases and the carbapenemases. Furthermore, the structure of PER-1 (a cephalosporinase) shows some major differences in the folding of some loops, in particular the Ω-loop, and the identity of some of the active-site residues (Tranier *et al.*, 2000). The defining difference between the penicillinases and the carbapenemases is the presence of the conserved disulfide bond in the active site in the latter subgroup and it has been postulated that the presence of this disulfide leads to the imipenemase activity of enzymes such as SME-1 (Swaren *et al.*, 1998; Sougakoff *et al.*, 2002). All members of the GES family of extended-spectum β-lactamases show the characteristics of the class A carbapenemases: primarily, the presence of the disulfide bond between Cys69 and Cys238. It is surprising therefore that several members of the family, including GES-1, lack the ability to hydrolyze carbapenems and are in fact inhibited by low concentrations of imipenem (Poirel *et al.*, 2000).

Since the isolation of GES-1 in 2000 (Poirel *et al.*, 2000), eight other members of the GES-type β-lactamase subfamily have been isolated, all of them point mutations of the original GES-1 enzyme (Fig. 3 and Table 4). All of these enzymes confer resistance to a number of β-lactam antibiotics, including the penicillins and some cephalosporins, including ceftazidime, and furthermore several of the enzymes have the ability to hydrolyse imipenem to an appreciable extent (Table 4). The determination of the three-dimensional structure of GES-1 now gives us an understanding of how the other members of the GES family have evolved carbapenemase activity.

The second GES enzyme to be isolated, IBC-1 (Giakkoupi *et al.*, 2000), later remaned GES-7 (Lee & Jeong, 2005), differs from GES-1 at two amino-acid positions: Glu104 is a lysine and Ala125 is a leucine. It has been suggested that a change from glutamate to lysine at position 104 could lower the K_m for substrates such as ceftazidime (Knox, 1995) and this appears to be the case for IBC-1/GES-7 (Table 4). Yet the observation that ceftazidime is a rather good substrate for GES-1 (k_{cat} = 380 s^{-1}) indicates that there are other factors involved in the activity of GES-1 towards this substrate. The second mutation at position 125 is about halfway along helix H4, facing towards helix H3 and partially exposed to solvent. This residue is over 10 Å from the active site and it is unlikely that this mutation in IBC-1/GES-7 plays any role in altering the activity of this variant. IBC-2 (later renamed GES-8), which was isolated around the same time, appears to be intermediate between IBC-1/GES-7 and GES-1 in that compared with GES-1 it only has once amino-acid change, leucine for alanine at position 125. Its resistance profile is very similar to GES-1 and shows no activity towards imipenem. This provides further verification that the change at position 125 has little or no effect on enzyme activity.

GES-2, isolated after IBC1/GES-7 (Poirel *et al.*, 2001), was found to have one amino-acid change compared with GES-1: an asparagine at position 170 instead of glycine. This mutation serves to shift the active site of GES-2 towards that of the other carbapenemases, such as NMC-A and SME-1, and produces a number of functional changes. The K_m for ceftazidime has increased and, more importantly, the K_m for imipenem has decreased by 100-fold, such that the GES-2 enzyme shows measurable hydrolytic activity towards the latter substrate. The majority of the β-lactamases have an asparagine at this position and, as noted above, this residue is involved in a hydrogen-bonding interaction with the hydrolytic water molecule and is generally thought to play a role in positioning the water prior to hydrolysis of the acyl-enzyme intermediate. The PER-1 enzyme (Tranier *et al.*, 2000) appears to be an exception, as it also has the Asn170 side chain missing. In this case, the change arises from the alteration in the conformation of the Ω-loop. PER-1 has a histidine at this position, the side chain of which is approximately 8 Å from the position occupied by Asn170 in the other class A β-lactamases. A glutamine residue at position 69 fulfills the role as the extra ligand for the hydrolytic water molecule in PER-1. This clearly is not the case in GES-1; based upon the current structural evidence, the hydrolytic water molecule is held in place by Ser70 and Glu166. It is conceivable that GES-1 might represent a more primitive form of the β-lactamase enzymes with a weakly held catalytic water molecule, which could presumably affect the rate of deacylation. The restoration of an asparagine at position 170 in GES-2 could provide an additional hydrogen bond to the hydrolytic water molecule and hold it more securely in the active site.

In order to ascertain what affect the Gly170Asn mutation might have on imipenem binding, the substrate was modeled into the active site of GES-1 using flexible-docking procedures and also into an *in silico* Gly170Asn mutant (called the 'GES-2' simulation). During the simulations, the side chains of the amino acids were free to adopt their favored rotamer conformations, as were the substituents on the imipenem substrate. The side chain of Glu166 was assumed to be protonated and the side chain of Lys73 was neutral. Docking of imipenem into the wild-type GES-1 active site (called the 'GES-1' simulation) and to 'GES-2' is shown in Fig. 5. In the 'GES-1' simulation, the substrate docks in roughly the same place as seen for the open-ring form of imipenem in TEM-1 (Maveyraud *et al.*, 1998). The carbonyl C atom of the β-lactam ring is 3.7 Å from Ser70 O^{γ}, a distance that is unfavorable for nucleophilic attack by the activated serine. The Ser70 side chain donates a hydrogen bond to the carbonyl O atom of the imipenem and receives a hydrogen bond from the hydrolytic water. The hydrolytic water both receives and donates a proton to the carboxylate of Glu166 in a classic bifurcated hydrogen bond. The most obvious change in the enzyme is the reorientation of Trp105. In the GES-1 structure, the side chain is oriented towards the C-terminus of helix H4 and is stabilized by a hydrogen-bonding interaction between the $N^{\varepsilon 1}$ atom and the carbonyl O atom of Leu124. In the 'GES-1' simulation, the Trp105 side chain has rotated by approximately 85° about the $C^{\alpha}-C^{\beta}$ bond (relative to the crystallographically observed rotamer) and flipped by 180° about the $C^{\beta}-C^{\gamma}$ bond. The indole ring now projects out into the solvent and stacks against the imipemen, coming within 4 Å of the five-membered ring. Compared with the imipenem complex with wild-type TEM-1 β-lactamase (Maveyraud *et al.*, 1998), the substrate in 'GES-1' has moved away from Ser70 and rotated about 20° down towards Trp105 and the O3 and O4 carboxylate O atoms sit deeper in the pocket occupied by the sulfate moiety. This reorientation is caused in part by the presence of the Thr237 side chain (this residue is an alanine in TEM-1) and is stabilized by hydrogen-bonding interactions with the side chain of Thr235. The rotation of the imipenem results in a marked reorientation of the aminomethylidene-amino-ethylsulfanyl tail and the formation of an electrostatic interaction between the terminal N atom of the imipenem and the side chain of Asp276 from the C-terminal region of helix H11. This residue is either aspartate or glutamate in all the known class A carbapenemases, yet shows wide variability in the penicillinases. It is possible that an acidic residue at this position may play a key role in positioning the imipenem correctly prior to deacylation and may result in the switch from imipenem being an inhibitor of the penicillinases to being a potential substrate for the carbapenemases.

In the 'GES-2' simulation, the side chain of the asparagine at position 170 forms a hydrogen-bonding interaction with the hydrolytic water and, as noted above, may serve to stabilize the water molecule in the active site. The imipenem molecule in 'GES-2' has moved approximately 1.5 Å out of the carboxylate-binding pocket towards the solvent. This brings the carbonyl O atom slightly closer to Ser70 O^{γ} (approximately 3.5 Å), but it is still too far away for nucleophilic attack by the serine. This might explain why both GES-1 and GES-2 have similar low k_{cat} values for imipenem (Table 4). The imipenem molecule in the 'GES-2' simulation makes several additional interactions with the protein compared with 'GES-1', which may help to explain the 100-fold difference in K_m between the variants. The hydroxyethyl group rotates by about 120° to present the hydroxyl group towards the side chain of Glu104, which in turn moves closer to the imipenem to form a hydrogen-bonding interaction. The carbonyl O atom of the imipenem is now much better positioned in the oxyanion hole and interacts with the amide N and carbonyl O atoms of Thr237 in addition to Ser70 O^{γ}. The interactions of the imipenem carboxylate moiety and the aminomethylideneamino-ethylsulfanyl tail are maintained and a new hydrogen bond is formed between the O4 atom and Ser130 O^{γ}. Although it is difficult to say why the presence of the Asn170 side chain might promote this movement of the imipenem, it does places the methyl group approximately 3.3–3.4 Å from the amide side chain of Asn170, where a nonpolar interaction between these groups might be favored.

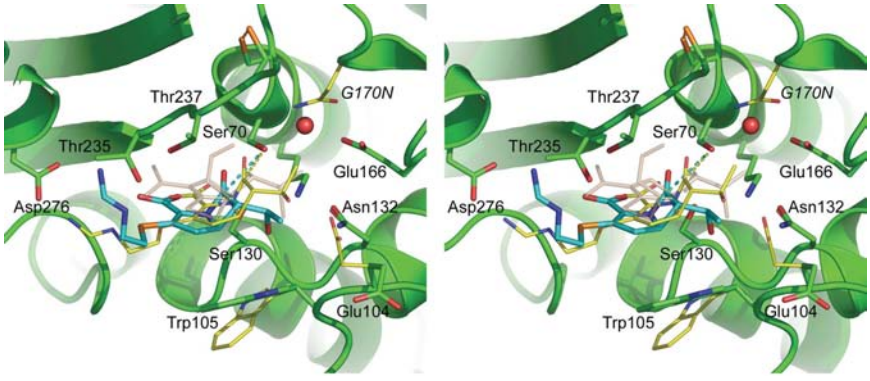

Figure 5
Stereoview of the 'GES-1' simulation active site (green) with the imipenem from 'GES-1' (cyan bonds) and 'GES-2' (thinner yellow bonds) superimposed. The imipenem from the wild-type TEM-1 β-lactamase complex (Maveyraud *et al.*, 1998) is shown in partially transparent cream bonds. In this case, the imipenem is in the hydrolyzed acyl-enzyme form. The large-scale movements of the Glu104 and Trp105 side chains are evident at the lower right of the figure, with the 'GES-1' rotamers in green and the 'GES-2' rotamers in thinner yellow bonds. The position of the G170N mutation in 'GES-2' is also indicated (yellow bonds) and would clearly interact with the hydrolytic water (red sphere) in this simulation. The cyan dashed line shows the long interaction distance between the carbonyl C atom of the docked 'GES-1' imipenem and the reactive Ser70 O^{γ} atom and the yellow dashed line shows the same interaction for the 'GES-2' imipenem.

The next four GES-type enzymes were identified at about the same time and led to confusion in the nomenclature, which was rectified by renaming the two enzymes discovered in a Greek hospital GES-5 and GES-6 (Vourli *et al.*, 2004) (Table 4), with the two enzymes characterized in Japan remaining as GES-3 (Wachino, Doi,

Yamane, Shibata, Yagi, Kubota, Ito *et al.*, 2004) and GES-4 (Wachino, Doi, Yamane, Shibata, Yagi, Kubota & Arakawa, 2004). GES-4 shows an increase in imipenem hydrolysis and a concomitant decrease in activity towards ceftazidime, primarily owing to a drop in k_{cat}. Both GES-3 and GES-4 have the Glu104Lys mutation observed in IBC-1/GES-7 and although in the latter enzyme this change appeared to result in a decrease in the ceftazidime K_m, the additional mutation Met62Thr in both GES-3 and GES-4 and the further change from glycine to serine at position 170 in GES-4 seems to counter this binding improvement to some extent (Table 4). More importantly, the Gly170Ser mutation in GES-4 confers significant activity towards imipenem and it would appear that the other two mutations have little or no effect on imipenemase activity. The K_m for GES-4 shows a tenfold increase relative to GES-2, but the k_{cat} has increased 100-fold. Furthermore, the GES-5 enzyme has recently been characterized (Bae *et al.*, 2007) and has a similar K_m for imipenem as GES-4 and a fourfold increase in k_{cat}. The same Gly170Ser mutation is present, but this variant does not have the changes at residues 62 and 104; it differs from GES-1 at position 170 only, thus confirming the conclusions drawn from the GES-3/GES-4 comparison that the Met62 and Glu104 mutations have no effect on imipenemase activity and may actually adversely affect the reaction rate.

Flexible-docking simulations on a Gly170Ser *in silico* mutant (the 'GES-5' simulation) show that the imipenem substrate would adopt a binding mode almost identical to that observed in the 'GES-1' simulation (not shown). The carbonyl C atom is again around 3.7 Å from Ser70 O^{γ} and the hydrogen-bonding interaction between the carbonyl O atom and Thr237 in the oxyanion hole is lost. The Trp105 side chain once again swings out towards the imipenem molecule. Based upon this simulation, it is difficult to account for the tenfold decrease in binding affinity in GES-5 compared with GES-1. This simulation also raises another important question: although the serine side chain at position 170 could make a hydrogen-bonding interaction with the hydrolytic water, would this really result in the observed 400-fold increase in k_{cat} in GES-5 given that everything else appears to be identical to GES-1? Furthermore, if this were the most important factor determining k_{cat}, why does GES-2 not show this same increase?

Although it is tempting to draw conclusions from these flexible-docking studies and attempt to correlate what is observed with the kinetic data, two important points should be kept in mind. Firstly, the K_m and k_{cat} values summarized in Table 4 were derived from several independent studies and may not be directly comparable since experimental design may differ from study to study. Secondly, it must be remembered that the simulations presented here relate to the binding of an intact imipemen molecule to the GES-1 model and as such may not necessarily reflect the true nature of the interaction of the substrate with the enzyme. The simulations might well mimic the initial approach of the intact β-lactam moiety into the active site, but a more complete understanding of all the factors affecting substrate binding in the GES-type enzymes must await further structural analyses of GES-1 and the point mutants GES-2 and GES-5.

4. Conclusions

The first crystal structure of a member of the GES-type family of class A extended-spectrum β-lactamases shows that these enzymes display the same structural features as other β-lactamase enzymes capable of hydrolyzing the 'magic bullet' carbapenem antibiotics, drugs that have for a long time been used as an antibiotic of last resort against multi-drug-resistant bacterial infections. The identity of the residue at position 170 appears to be highly critical for imipenemase activity. Clearly, it is not just the presence of the disulfide bond which confers carbapenemase activity on these enzymes and something a little more subtle is happening in the active site involving the interplay of a number of residues, most certainly including residue 170. The nature of this residue is very important, since in all other penicillinases and carbapenemases it is invariably asparagine and when this residue is changed to a glycine, as in GES-1, what looks like an enzyme potentially capable of hydrolyzing impenem fails to show that activity. More importantly, perhaps, the presence of imipenemase activity in the GES-type enzymes involves changes at this very position, either to the idiosyncratic asparagine or to a serine.

It has to be remembered, however, that the order in which the GES-type enzymes were isolated and characterized probably bears little relation to the order in which these variants may have emerged and it impossible at this stage to categorically state which of the GES variants is the prototypical enzyme from which the others could have evolved. It is really only possible to compare the variants individually and gain some understanding as to why a particular member displays a certain resistance profile and what changes in other variants produce their specific activity. Whether we are observing a slowly evolving carbapenamase activity in the GES-type class A β-lactamases must await further studies.

References

Ambler, R. P., Coulson, A. F. W., Frere, J. M., Ghuysen, J. M., Joris, B., Forsman, M., Levesque, R. C., Tiraby, G. & Waley, S. G. (1991). *Biochem. J.* **276**, 269–270.

Bae, I. K., Lee, Y. N., Jeong, S. H., Hong, S. G., Lee, J. H., Lee, S. H., Kim, H. J. & Youn, H. (2007). *Diag. Microbiol. Infect. Dis.* doi:10.1016/j.diagmicrobio.2007.02.013.

Bartlett, J. G. (2003). *Pocket Book of Infectious Disease Therapy*. Baltimore: Lippincott Williams & Wilkins.

Chen, C. C. & Herzberg, O. (1992). *J. Mol. Biol.* **224**, 1103–1113.

Chen, C. C. & Herzberg, O. (2001). *Biochemistry*, **40**, 2351–2358.

Chen, Y., Delmas, J., Sirot, J., Shoichet, B. & Bonnet, R. (2005). *J. Mol. Biol.* **348**, 349–362.

Collaborative Computational Project, Number 4 (1994). *Acta Cryst.* D**50**, 760–763.

DeLano, W. L. (2002). *The PyMOL Molecular Graphics System.* http://www.pymol.org.

Emsley, P. & Cowtan, K. (2004). *Acta Cryst.* D**60**, 2126–2132.

Giakkoupi, P., Tzouvelekis, L. S., Tsakris, A., Loukova, V., Sofianou, D. & Tzelepi, E. (2000). *Antimicrob. Agents Chemother.* **44**, 2247–2253.
Jacoby, G. & Bush, K. (2007). *Amino-Acid Sequences for TEM, SHV and OXA Extended-Spectrum and Inhibitor-Resistant β-Lactamases.* http://www.lahey.org/studies/webt.asp.
Jelsch, C., Mourey, L., Masson, J. M. & Samama, J. P. (1993). *Proteins*, **16**, 364–383.
Kabsch, W. (1993). *J. Appl. Cryst.* **26**, 795–800.
Ke, W., Bethel, C. R., Thomson, J. M., Bonomo, R. A. & van den Akker, F. (2007). *Biochemistry*, **46**, 5732–5740.
Knox, J. R. (1995). *Antimicrob. Agents Chemother.* **39**, 2593–2601.
Knox, J. R. & Moews, P. C. (1991). *J. Mol. Biol.* **220**, 435–455.
Krissinel, E. & Henrick, K. (2004). *Acta Cryst.* D**60**, 2256–2268.
Lee, S. H. & Jeong, S. H. (2005). *Antimicrob. Agents Chemother.* **49**, 2148–2150.
Livermore, D. M. & Woodford, N. (2006). *Trends Microbiol.* **14**, 413–420.
Matthews, B. W. (1968). *J. Mol. Biol.* **33**, 491–497.
Maveyraud, L., Mourey, L., Kotra, L. P., Pedelacq, J. D., Guillet, V., Mobashery, S. & Samama, J. P. (1998). *J. Am. Chem. Soc.* **120**, 9748–9752.
Mavroidi, A., Tzelepi, E., Tsakris, A., Miriagou, V., Sofianou, D. & Tzouvelekis, L. S. (2001). *J. Antimicrob. Chemother.* **48**, 627–630.
Merritt, E. A. (1999). *Acta Cryst.* D**55**, 1109–1117.
Minasov, G., Wang, X. & Shoichet, B. K. (2002). *J. Am. Chem. Soc.* **124**, 5333–5340.
Murray, J. W., Garman, E. F. & Ravelli, R. B. G. (2004). *J. Appl. Cryst.* **37**, 513–522.
Murshudov, G. N., Vagin, A. A., Lebedev, A., Wilson, K. S. & Dodson, E. J. (1999). *Acta Cryst.* D**55**, 247–255.
Nukaga, M., Abe, T., Venkatesan, A. M., Mansour, T. S., Bonomo, R. A. & Knox, J. R. (2003). *Biochemistry*, **42**, 13152–13159.
Nukaga, M., Mayama, K., Crichlow, G. V. & Knox, J. R. (2002). *J. Mol. Biol.* **317**, 109–117.
Nukaga, M., Mayama, K., Hujer, A. M., Bonomo, R. A. & Knox, J. R. (2003). *J. Mol. Biol.* **328**, 289–301.
Otwinowski, Z. & Minor, W. (1997). *Methods Enzymol.* **276**, 307–326.
Owen, R. L., Rudiño-Piñera, E. & Garman, E. F. (2006). *Proc. Natl Acad. Sci. USA*, **103**, 4912–4917.
Park, S., Morley, K. L., Horsman, G. P., Holmquist, M., Hult, K. & Kazlauskas, R. J. (2005). *Chem. Biol.* **12**, 45–54.
Poirel, L., Brinas, L., Fortineau, N. & Nordmann, P. (2005). *Antimicrobial Agents Chemother.* **49**, 3593–3597.
Poirel, L., Le Thomas, I., Naas, T., Karim, A. & Nordmann, P. (2000). *Antimicrob. Agents Chemother.* **44**, 622–632.
Poirel, L., Weldhagen, G. F., Naas, T., De Champs, C., Dove, M. G. & Nordmann, P. (2001). *Antimicrob. Agents Chemother.* **45**, 2598–2603.
Poole, K. (2004). *Cell. Mol. Life Sci.* **61**, 2200–2223.
Schapira, M., Abagyan, R. & Totrov, M. (2003). *J. Med. Chem.* **46**, 3045–3059.
Schapira, M., Raaka, B. M., Das, S., Fan, L., Totrov, M., Zhou, Z., Wilson, S. R., Abagyan, R. & Samuels, H. H. (2003). *Proc. Natl Acad. Sci. USA*, **100**, 7354–7359.
Sheldrick, G. M. & Schneider, T. R. (1997). *Methods Enzymol.* **227**, 319–343.
Siu, L. K. (2002). *J. Microbiol. Immunol. Infect.* **35**, 1–11.
Sougakoff, W., L'Hermite, G., Pernot, L., Naas, T., Guillet, V., Nordmann, P., Jarlier, V. & Delettré, J. (2002). *Acta Cryst.* D**58**, 267–274.
Strynadka, N. C. J., Adachi, H., Jensen, S. E., Johns, K., Sielecki, A., Betzel, C., Sutoh, K. & James, M. N. G. (1992). *Nature (London)*, **359**, 700–705.
Swaren, P., Maveyraud, L., Raquet, X., Cabantous, S., Duez, C., Pedelacq, J. D., Mariotte-Boyer, S., Mourey, L., Labia, R., Nicolas-Chanoine, M. H., Nordmann, P., Frere, J. M. & Samama, J. P. (1998). *J. Biol. Chem.* **273**, 26714–26721.
Tranier, S., Bouthors, A. T., Maveyraud, L., Guillet, V., Sougakoff, W. & Samama, J. P. (2000). *J. Biol. Chem.* **275**, 28075–28082.
Vourli, S., Giakkoupi, P., Miriagou, V., Tzelepi, E., Vatopoulos, A. C. & Tzouvelekis, L. S. (2004). *FEMS Microbiol. Lett.* **234**, 209–213.
Wachino, J., Doi, Y., Yamane, K., Shibata, N., Yagi, T., Kubota, T. & Arakawa, Y. (2004). *Antimicrob. Agents Chemother.* **48**, 2905–2910.
Wachino, J., Doi, Y., Yamane, K., Shibata, N., Yagi, T., Kubota, T., Ito, H. & Arakawa, Y. (2004). *Antimicrob. Agents Chemother.* **48**, 1960–1967.
Wang, X., Minasov, G. & Shoichet, B. K. (2002). *Proteins*, **47**, 86–96.